

LDPC codes for the Cascaded BSC-BAWGN channel

Aravind R. Iyengar, Paul H. Siegel, and Jack K. Wolf

University of California, San Diego
9500 Gilman Dr. La Jolla CA 92093

email: {aravind,psiegel,jwolf}@ucsd.edu

Abstract—We study the performance of LDPC codes over the cascaded BSC-BAWGN channel. This channel belongs to a family of binary-input, memoryless, symmetric-output channels, one that we call the $\{\text{CBMSC}(p, \sigma)\}$ family. We analyze the belief propagation (BP) decoder over this channel by characterizing the decodable region of an ensemble of LDPC codes. We then give inner and outer bounds for this decodable region based on existing universal bounds on the performance of a BP decoder. We numerically evaluate the decodable region using density evolution. We also propose other message-passing schemes of interest and give their decodable regions. The performance of each proposed decoder over the CBMS channel family is evaluated through simulations. Finally, we explore capacity-approaching LDPC code ensembles for the $\{\text{CBMSC}(p, \sigma)\}$ family.

I. INTRODUCTION

Low-density parity-check (LDPC) codes [1], [2] have been shown to achieve performance close to capacity over binary-input, memoryless, symmetric-output (BMS [3]) channels like the binary erasure channel (BEC) [4], the binary symmetric channel (BSC) [5] and the binary-input additive white Gaussian noise channel (BAWGNC) [5], [6], [7]. We consider a class of channels which belong to the same BMS channel family as the BEC, BSC and BAWGNC. Owing to this similarity, much of the terminology and notation used in this paper are reminiscent of the analysis of LDPC ensemble performance in [3]. However, the channels under consideration exhibit certain differences from the BMS channels in [3] because of their multidimensional channel space.

This paper is organized as follows. In Section II, we introduce the $\text{CBMS}(p, \sigma)$ channel family and discuss some characteristics of this family of channels. We then consider coding over this channel using LDPC codes and analyze the belief propagation (BP) decoder in Section III. On similar lines, we propose and analyze two other message-passing schemes in Section IV. We give experimental results for the performance of the three message-passing decoders in Section V. In Section VI, we explore good LDPC codes for the $\text{CBMS}(p, \sigma)$ channel. We conclude by summarizing our findings in Section VII.

II. THE CHANNEL MODEL

A. Cascaded channels

A cascaded channel is one where the output of one channel is fed as input to another. The constituent channels of a cascaded channel are called *subchannels*. The input of the cascaded channel is the input to its first subchannel, and the

output is the output of the last subchannel in the cascade. The outputs (resp. inputs) of all subchannels other than the last (resp. first) are inaccessible. Note that from the definition, it follows that two subchannels can be cascaded only if the output alphabet of the first is the same as the input alphabet of the next. We will assume that the cascaded channel consists of only two subchannels. A generalization to an arbitrary number of subchannels is straightforward.

Further, we will call a cascaded channel a *cascaded BMS* (CBMS) channel if it is a cascade of a BMS channel with a memoryless, symmetric channel. It is easy to see that any CBMS channel is symmetric and memoryless. Since the input to a CBMS channel is binary, CBMS channels belong to the family of BMS channels. However, unlike simple BMS channels¹, CBMS channels are parameterized by the fidelities of both the constituent subchannels.

We note here that a CBMS channel could be a degraded BMS channel belonging to the same channel family as the first subchannel [8], e.g. a BAWGN channel followed by another AWGN channel will give a CBMS channel which is also a BAWGN channel with a larger noise variance. In this case the CBMS channel is in the same family as the first subchannel. However, a BAWGN channel followed by a Laplace channel is also a CBMS channel, one not belonging to the family of BAWGN channels.

B. Cascaded BSC-BAWGN channel

The cascaded BSC-BAWGN channel, as the name suggests, is a CBMS channel where the first subchannel is a BSC with crossover probability p and the second subchannel is a BAWGNC with noise variance σ^2 . It is denoted as $\text{CBMSC}(p, \sigma)$ and is depicted in Figure 1. Note that the

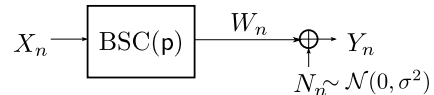


Fig. 1. The $\text{CBMSC}(p, \sigma)$ channel.

channel space for this channel is given as $\mathcal{S} = [0, 1/2] \times \mathbb{R}^+$. The family of channels over \mathcal{S} is denoted $\{\text{CBMSC}(p, \sigma)\}$.

The capacity of cascaded channels has been considered under certain cases of interest in [9], [10], [11], [12]. Since

¹We will refer to BMS channels parameterized by a single variable as *simple* BMS channels.

the $\text{CBMS}(p, \sigma)$ channels are BMS channels, the capacity of the family of these channels can be numerically evaluated [3]. Figure 2 shows the contours of equal capacity² in a subset of \mathcal{S} . Though we write the parameters of the channel as the ordered pair (p, σ) in accordance with the order of the subchannels, all figures in this paper are depicted with p as the ordinate for convenience. Note that the extremal

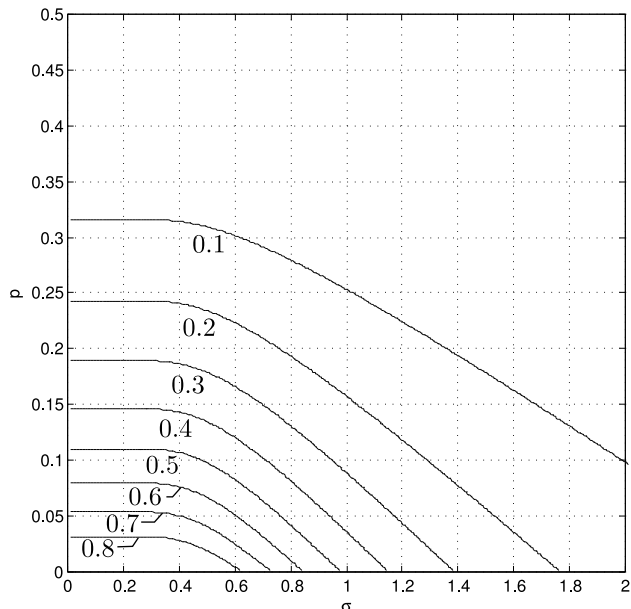


Fig. 2. Contours of Capacity $\mathcal{C}(p, \sigma)$ of the family $\{\text{CBMSC}(p, \sigma)\}$ in bits per channel use.

channels in this family correspond to the families $\{\text{BSC}(p)\}$ and $\{\text{BAWGNC}(\sigma)\}$ when $\sigma = 0$ and $p = 0$ respectively.

C. Motivation

The motivation for considering the $\text{CBMS}(p, \sigma)$ channel family comes from a new-generation magnetic recording media called *bit patterned media* (BPM). BPM is claimed to surpass conventional magnetic recording media in storage capacities owing to its structure. The superparamagnetic effect that makes it difficult to reduce the size of bit cells in conventional media is avoided by storing bits on magnetic islands isolated by non-magnetic material. However, this structure brings to fore the challenge of good timing and positional synchronization of the write head during the write process. There is therefore a possibility of writing data erroneously on the disk [13]. We model this *write channel* as a BSC, which is followed by a memoryless *read channel* modelled as a BAWGNC. The $\text{CBMS}(p, \sigma)$ channel therefore serves as a first-order approximation of the BPM channel – the (coded) information X_n (See Figure 1) gets written onto the disk as W_n , which is then read as Y_n . A more realistic model would be a similar write and read channel cascade where the subchannels have memory, which is a subject for future work.

²Throughout the paper, we will assume that information theoretic quantities like entropy and capacity are measured in terms of bits.

The $\text{CBMS}(p, \sigma)$ channel can also model other scenarios like an earth-satellite-earth link with a simplistic hard-decision decoder on the satellite and a more powerful soft-decision decoder at the receiver on the earth. In general, all memoryless (multihop) relay channels with thresholding at intermediate nodes can be modeled as $\text{CBMS}(p, \sigma)$ channels.

D. Coding for the $\text{CBMS}(p, \sigma)$ channel

Owing to the asymptotically close-to-optimal performance of LDPC codes over the subchannels of the $\text{CBMS}(p, \sigma)$ channel, we will consider coding for the $\text{CBMS}(p, \sigma)$ channel using LDPC codes and the performance of these codes with iterative message-passing decoders with emphasis on the asymptotically bit-optimal BP decoder.

Note that since message-passing schemes are in general hypothesized on some channel model, estimation of channel parameters plays a key role in decoding. In this case, this translates to the availability of good estimates for p and the SNR (defined in dB as $\text{SNR} := -20 \log \sigma$) of the constituent subchannels of the $\text{CBMS}(p, \sigma)$ channel, which will be assumed.

III. THE BELIEF PROPAGATION DECODER

Since the $\text{CBMS}(p, \sigma)$ channel is a BMS channel, the Log-Likelihood Ratio (LLR) of the channel output is a sufficient statistic for decoding [3]. The BP decoding scheme thus remains the same as in the case of simple BMS channels, except for the initial channel LLR density. Hence, the analysis of the BP decoder over the $\text{CBMS}(p, \sigma)$ channel can be performed using the standard density evolution [3], [6], [8] of the LLR of the channel output, i.e. the convergence to the tree channel, the restriction to the all-zero codeword and the concentration around the ensemble average arguments [3] can be carried forward to this case. In this case, we have the LLR l to be

$$l = \ln \left[\frac{(1-p)e^{\tilde{l}} + p}{(1-p) + pe^{\tilde{l}}} \right] \quad (1)$$

where $\tilde{l} = 2y/\sigma^2$, a function of the channel output y . Note that in case of a BAWGNC, \tilde{l} gives the actual LLR (which can be readily seen by setting $p = 0$).

We fix a code ensemble [3] (λ, ρ) , and define the *decodable region* of the ensemble as

$$\mathcal{R}_{(\lambda, \rho)} := \left\{ (p, \sigma) : \mathbb{P}_{(\lambda, \rho)}^{(p, \sigma)} = 0 \right\} \quad (2)$$

where $\mathbb{P}_{(\lambda, \rho)}^{(p, \sigma)}$ denotes the probability that the message on a random edge of the Tanner graph of a code in the ensemble (λ, ρ) is in error, averaged over the ensemble, in the limit of infinite blocklength and infinite rounds of message-passing. The boundary of the decodable region is analogous to the *threshold* value of simple BMS channels [3], [8].

Whereas in the case of simple BMS channels the channel families are *totally ordered* by *degradation* [8], the $\{\text{CBMSC}(p, \sigma)\}$ channel family is only *partially ordered* by degradation. We therefore devote attention to characterizing and bounding the decodable region of an LDPC code ensemble

for the family of CBMS(ρ, σ) channels. For completeness, we revisit the definition of degradation.

Definition 1 (Degraded channels): A channel $Z|X$ is output degraded with respect to $Y|X$ if $X \rightarrow Y \rightarrow Z$, i.e. X, Y and Z form a Markov chain.

A. Characterization of $\mathcal{R}_{(\lambda, \rho)}$

The following can be deduced directly from the channel degradation argument of [8].

Lemma 1 (Monotonicity in σ): If $(\rho, \sigma) \in \mathcal{R}_{(\lambda, \rho)}$, then $(\rho, \underline{\sigma}) \in \mathcal{R}_{(\lambda, \rho)} \forall \underline{\sigma} \leq \sigma$.

In order to prove a similar monotonicity in the parameter ρ , we construct a channel that is equivalent to the CBMS(ρ, σ) channel, but is degraded with respect to BAWGNC(σ). Note that it is not immediately obvious that the CBMS(ρ, σ) channel, as in Figure 1, is output degraded with respect to BAWGNC(σ).

Definition 2 (Input-distorted channels): Let $X \rightarrow Y$ be a BSC with crossover probability ρ , and let $Y \rightarrow Z$ be any BMS channel with transition probability $f_{Z|Y}$. Then the channel $Z|X$ is said to be input-distorted with respect to the channel $Z|Y$.

Note that any CBMS channel with its second subchannel being a BMS channel itself is an input-distorted channel by definition.

Theorem 1 (Equivalence of input-distortion & degradation): Any input-distorted channel $X \rightarrow Y \rightarrow Z$ is degraded with respect to the channel $Y \rightarrow Z$.

Proof: By definition, we have $X \in \mathcal{X} = \{\pm 1\}$, $Y \in \mathcal{Y} = \mathcal{X}$, $f_{Y|X}(y|x) = (1 - \rho)\delta(y - x) + \rho\delta(y + x)$ for some $\rho \in [0, 1/2]$, where $\delta(x) = \begin{cases} 1 & x = 0 \\ 0 & \text{else} \end{cases}$, and $f_{Z|Y}(-z|y) = f_{Z|Y}(z|y)$. Then,

$$\begin{aligned} f_{Z|X}(z|x) &= \sum_{y \in \mathcal{Y}} f_{Y,Z|X}(y, z|x) \\ &= \sum_{y \in \mathcal{Y}} f_{Y|X}(y|x) f_{Z|Y}(z|y) \\ &= \sum_{y \in \mathcal{Y}} \{(1 - \rho)\delta(y - x) + \rho\delta(y + x)\} f_{Z|Y}(z|y) \\ &= (1 - \rho) f_{Z|Y}(z|x) + \rho f_{Z|Y}(z|-x) \\ &= (1 - \rho) f_{Z|Y}(z|x) + \rho f_{Z|Y}(-z|x) \end{aligned} \quad (3)$$

Consider the channel system $Y \rightarrow Z \rightarrow W$ where the channel $Y \rightarrow Z$ is given as before, and the channel $Z \rightarrow W$ satisfies $W \in \mathcal{W} = \mathcal{Z}$ and $f_{W|Z}(w|z) = (1 - \rho)\delta(w - z) + \rho\delta(w + z)$. Then

$$\begin{aligned} f_{W|Y}(w|y) &= \int_{z \in \mathcal{Z}} f_{Z,W|Y}(z, w|y) dz \\ &= \int_{z \in \mathcal{Z}} f_{Z|Y}(z|y) f_{W|Z}(w|z) dz \\ &= (1 - \rho) f_{Z|Y}(w|y) + \rho f_{Z|Y}(-w|y) \end{aligned} \quad (4)$$

From (3) and (4), we have $f_{Z|X} = f_{W|Y}$. Since the channel $Y \rightarrow Z$ degrades to $Y \rightarrow W$, we conclude that $Y \rightarrow Z$ degrades to $X \rightarrow Z$. ■

From Theorem 1 and the channel degradation argument of [8], we have the following lemma

Lemma 2 (Monotonicity in ρ): If $(\rho, \sigma) \in \mathcal{R}_{(\lambda, \rho)}$, then $(\underline{\rho}, \sigma) \in \mathcal{R}_{(\lambda, \rho)} \forall \underline{\rho} \leq \rho$.

A consequence of Lemmas 1 and 2 is that if a point (ρ, σ) is found to be in $\mathcal{R}_{(\lambda, \rho)}$, then we can conclude that all channel points with a smaller σ and a smaller ρ (points to the left and below (ρ, σ) in the channel space \mathcal{S}) are also guaranteed to belong to $\mathcal{R}_{(\lambda, \rho)}$.

B. Bounds for $\mathcal{R}_{(\lambda, \rho)}$

We now give inner and outer bounds for the decodable region of a code ensemble based on existing universal bounds on the performance of the BP decoder.

Proposition 1 (Bhattacharyya outer bound): Let $\bar{\mathcal{B}}_{(\lambda, \rho)} = \{(\rho, \sigma) \in \mathcal{S} : \mathbb{B}(\rho, \sigma) < \mathbb{B}_{(\lambda, \rho)}^*\}$, where $\mathbb{B}(\rho, \sigma)$ is the *Bhattacharyya constant* [3] associated with the channel CBMSC(ρ, σ) and $\mathbb{B}_{(\lambda, \rho)}^* := \inf\{\bar{b}(x) : \bar{b}(x) \geq x, x \in (0, 1]\}$, with

$$\bar{b}(x) = \frac{x}{\lambda \left(\sum_k \rho_k \sqrt{1 - (1 - x^2)^{k-1}} \right)}.$$

Then, $\mathcal{R}_{(\lambda, \rho)} \subset \bar{\mathcal{B}}_{(\lambda, \rho)}$.

Discussion This follows from the universal upper bound on the Bhattacharyya constant given in [14], [15]. First, any BMS channel is expressed as a convex combination of BSCs of crossover probabilities ranging from 0 to 1/2. Noting that the check node processing for a density corresponding to a BSC gives the smallest Bhattacharyya constant for the output density, the above upper bound on the Bhattacharyya parameter can be obtained.

Proposition 2 (Entropy outer bound): Let $\bar{\mathcal{H}}_{(\lambda, \rho)} = \{(\rho, \sigma) \in \mathcal{S} : \mathbb{H}(\rho, \sigma) < \mathbb{H}_{(\lambda, \rho)}^*\}$, where $\mathbb{H}(\rho, \sigma)$ is the *entropy (channel equivocation)* [3], [8], [16] associated with the channel CBMSC(ρ, σ) and $\mathbb{H}_{(\lambda, \rho)}^* := \inf\{\bar{h}(x) : \bar{h}(x) \geq x, x \in (0, 1/2]\}$, with

$$\bar{h}(x) = \frac{h_2(x)}{\lambda \left(\sum_k \rho_k h_2 \left(\frac{1 + (1 - 2x)^{k-1}}{2} \right) \right)},$$

where $h_2(\cdot)$ is the *binary entropy function*. Then, $\mathcal{R}_{(\lambda, \rho)} \subset \bar{\mathcal{H}}_{(\lambda, \rho)}$.

Discussion This follows from the best case of the ‘‘extremes of information combining’’ [16]. As in Proposition 1, the smallest entropy of the output density is obtained for input densities corresponding to BSC at the check node and BEC at the variable node. Using these best case densities, we obtain the upper bound for the entropy.

Proposition 3 (Capacity outer bound): Let $\bar{\mathcal{C}}_{(\lambda, \rho)} := \{(\rho, \sigma) \in \mathcal{S} : \mathbb{C}(\rho, \sigma) > \mathfrak{r}(\lambda, \rho)\}$ where $\mathbb{C}(\rho, \sigma)$ is the capacity of the channel CBMSC(ρ, σ) and $\mathfrak{r}(\lambda, \rho) = 1 - \frac{\int_0^1 \rho(x) dx}{\int_0^1 \lambda(x) dx}$ is the *design rate* of the code. Then $\mathcal{R}_{(\lambda, \rho)} \subset \bar{\mathcal{C}}_{(\lambda, \rho)}$.

Proof: Since the asymptotic (in blocklength) actual rate r of a code is equal to its design rate \mathfrak{r} [3], the result follows from the channel coding theorem. ■

Proposition 4 (Degradation outer bound): Let $\bar{\mathcal{D}}_{(\lambda,\rho)} = \{(\mathbf{p}, \sigma) \in \mathcal{S} : \sigma < \sigma_{(\lambda,\rho)}^*, \mathbf{p} < \mathbf{p}_{(\lambda,\rho)}^*\}$, where $\sigma_{(\lambda,\rho)}^*$ is the threshold for the (λ, ρ) code ensemble over the family $\{\text{BAWGNC}(\sigma)\}$, and $\mathbf{p}_{(\lambda,\rho)}^*$ is that over the family $\{\text{BSC}(\mathbf{p})\}$. Then, $\mathcal{R}_{(\lambda,\rho)} \subset \bar{\mathcal{D}}_{(\lambda,\rho)}$.

Proof: Suppose to the contrary that $\mathbb{P}_{(\lambda,\rho)}^{(\mathbf{p},\sigma)} = 0$ for some $\sigma > \sigma_{(\lambda,\rho)}^*$. Then, since $\text{BAWGNC}(\sigma)$ degrades to $\text{CBMSC}(\mathbf{p}, \sigma)$, we have $\mathbb{P}_{(\lambda,\rho)}^{(\sigma,0)} = 0 \Rightarrow (\sigma, 0) \in \mathcal{R}_{(\lambda,\rho)}$ which contradicts the assumption that $\sigma_{(\lambda,\rho)}^*$ is the threshold for the BAWGN channel family. A similar argument holds for $\mathbf{p}_{(\lambda,\rho)}^*$.

This bound is more easily stated as the contrapositive of the claims made in Lemmas 1 and 2. ■

Figure 3 shows the outer bounds discussed here for two code ensembles. The set $\bar{\mathcal{B}}_{(\lambda,\rho)} \cap \bar{\mathcal{H}}_{(\lambda,\rho)} \cap \bar{\mathcal{C}}_{(\lambda,\rho)} \cap \bar{\mathcal{D}}_{(\lambda,\rho)}$ is therefore an outer bound for the decodable region. We have observed that the Bhattacharyya bound and the entropy bound have been strictly looser than the capacity bound in all cases we considered, with the Bhattacharyya bound being the loosest.

Proposition 5 (Bhattacharyya inner bound): Let $\underline{\mathcal{B}}_{(\lambda,\rho)} = \{(\mathbf{p}, \sigma) \in \mathcal{S} : \text{B}(\mathbf{p}, \sigma) < \text{B}'_{(\lambda,\rho)}\}$, where $\text{B}'_{(\lambda,\rho)} := \inf\{\underline{b}(x) : \underline{b}(x) \geq x, x \in (0, 1]\}$, with

$$\underline{b}(x) = \frac{x}{\lambda(1 - \rho(1 - x))}.$$

Then, $\underline{\mathcal{B}}_{(\lambda,\rho)} \subset \mathcal{R}_{(\lambda,\rho)}$.

Discussion This follows from the universal lower bound on the Bhattacharyya constant of a BMS channel [14], [15]. In this case, the lower bound is obtained as in Proposition 1, by noting that the check node processing for a density corresponding to a BEC gives the largest Bhattacharyya constant for the output density.

Note that the above bound is tight for the BEC, in which case the Bhattacharyya constant is given by the channel erasure probability. The above definition of $\text{B}'_{(\lambda,\rho)}$ therefore coincides with the definition of the threshold for the BEC in [3], [8].

Proposition 6 (Entropy inner bound): Let $\underline{\mathcal{H}}_{(\lambda,\rho)} = \{(\mathbf{p}, \sigma) \in \mathcal{S} : \text{H}(\mathbf{p}, \sigma) < \text{H}'_{(\lambda,\rho)}\}$, where $\text{H}'_{(\lambda,\rho)} := \inf\{h_2(\mathbf{p}), \mathbf{p} \in (0, 1/2) : \exists x \in (0, 1/2) : \underline{h}(x, \mathbf{p}) \geq 0\}$, with

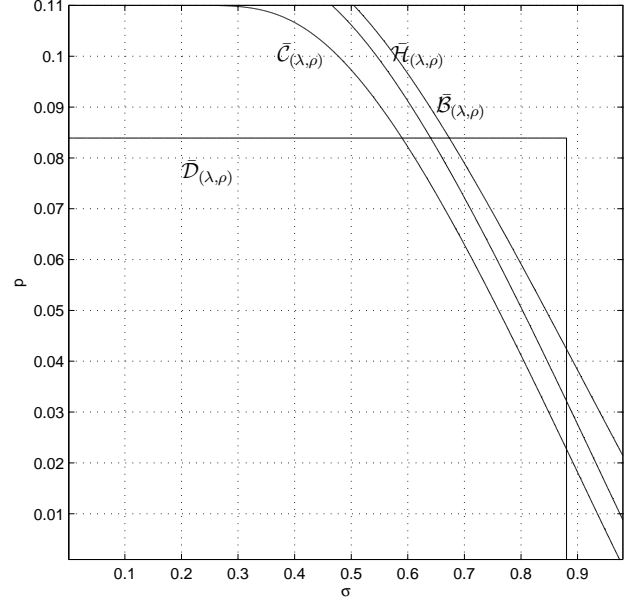
$$\underline{h}(x, \mathbf{p}) = 1 - h_2(x) - \rho(1 - \hat{h}(\lambda, x, \mathbf{p})),$$

$$\hat{h}(\lambda, x, \mathbf{p}) = \sum_j \lambda_j \sum_{l=0}^{j-1} \binom{j-1}{l} x^l (1-x)^{j-1-l} \tilde{h}(\mathbf{p}, x, j, l),$$

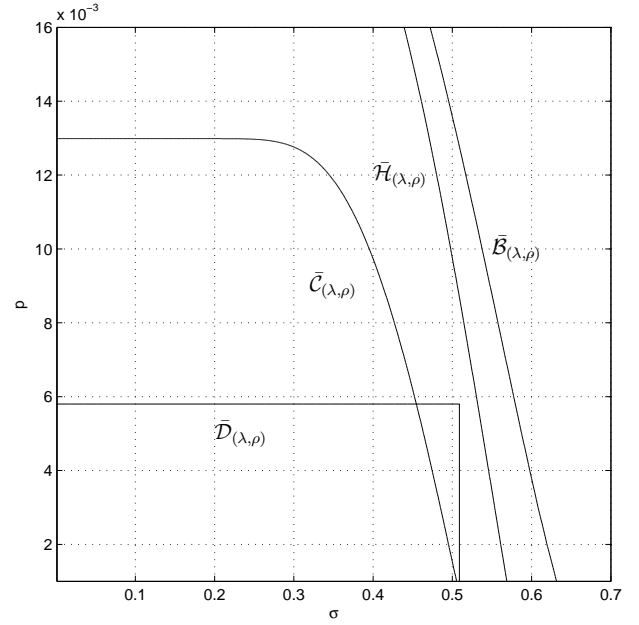
and $\tilde{h}(\mathbf{p}, x, j, l)$ as in (5). Then, $\underline{\mathcal{H}}_{(\lambda,\rho)} \subset \mathcal{R}_{(\lambda,\rho)}$.

Discussion This follows from the worst case of the “extremes of information combining” [16]. As in Proposition 2, the lower bound is obtained by noting that the largest entropy of the output density is obtained for input densities corresponding to BEC at the check node and BSC at the variable node.

Proposition 7 (Degradation inner bound): Let $\underline{\mathcal{D}}_{(\lambda,\rho)} = \{(\mathbf{p}, \sigma) \in \mathcal{S} : \mathbf{p} \star Q(\frac{1}{\sigma}) < \mathbf{p}_{(\lambda,\rho)}^*\}$ where $\mathbf{p}_{(\lambda,\rho)}^*$ is as in Proposition 4, $a \star b = a(1-b) + b(1-a)$, $\forall a, b \in [0, 1/2]$



(a) (3, 6) regular code ensemble – $\lambda(x) = x^2, \rho(x) = x^5$.



(b) Rate-0.9 code ensemble optimized[5] for the BAWGNC – $\lambda(x) = 0.440212x^{14} + 0.0529353x^5 + 0.126393x^4 + 0.231598x^2 + 0.148861x, \rho(x) = 0.5x^{46} + 0.5x^{45}$, henceforth referred to as the “Optimized rate-0.9 code ensemble.”

Fig. 3. Outer bounds for the decodable region $\mathcal{R}_{(\lambda,\rho)}$. The sets correspond to the region under the curves marked in the figure.

and $Q(\cdot)$ is the Q-function of the standard normal distribution. Then, $\underline{\mathcal{D}}_{(\lambda,\rho)} \subset \mathcal{R}_{(\lambda,\rho)}$.

Proof: Let $X \rightarrow Y \rightarrow Z$ be the CBMS(\mathbf{p}, σ) channel. Consider the channel $X \rightarrow Y \rightarrow Z \rightarrow W$, where $W = \text{sgn}(Z) = \begin{cases} +1, & Z \geq 0 \\ -1, & Z < 0 \end{cases}$. We have $W \in \mathcal{W} = \{\pm 1\} = \mathcal{X}$, and $p_{W|X}(w|x) = (1 - \mathbf{p}')\delta(w - x) + \mathbf{p}'\delta(w + x)$, with $\mathbf{p}' = \mathbf{p} \star Q(\frac{1}{\sigma})$. Thus, $X \rightarrow W$ is a BSC with crossover probability \mathbf{p}' . Thus, if $\mathbf{p}' < \mathbf{p}_{(\lambda,\rho)}^*$, the threshold for the family $\{\text{BSC}(\mathbf{p})\}$,

$$\tilde{h}(\mathbf{p}, x, j, l) = \mathbf{p} \log_2 \left[1 + \frac{1-\mathbf{p}}{\mathbf{p}} \left(\frac{x}{1-x} \right)^{j-1-2l} \right] + (1-\mathbf{p}) \log_2 \left[1 + \frac{\mathbf{p}}{1-\mathbf{p}} \left(\frac{x}{1-x} \right)^{j-1-2l} \right]. \quad (5)$$

we have $\mathbb{P}_{(\lambda, \rho)}^{\mathbf{p}'}$ = 0. Since the channel $X \rightarrow Z$ degrades to the channel $X \rightarrow W$, $\mathbb{P}_{(\lambda, \rho)}^{\mathbf{p}'} = 0 \Rightarrow \mathbb{P}_{(\lambda, \rho)}^{(\mathbf{p}, \sigma)} = 0$. Hence, if $(\mathbf{p}, \sigma) \in \underline{\mathcal{D}}_{(\lambda, \rho)}$, then $(\mathbf{p}, \sigma) \in \mathcal{R}_{(\lambda, \rho)}$. ■

Proposition 8 (Soft bit inner bound): Let $\underline{\mathcal{S}}_{(\lambda, \rho)} = \left\{ (\mathbf{p}, \sigma) \in \mathcal{S} : \mathbf{S}(\mathbf{p}, \sigma) < 4\mathbf{p}_{(\lambda, \rho)}^*(1 - \mathbf{p}_{(\lambda, \rho)}^*) \right\}$ where $\mathbf{S}(\mathbf{p}, \sigma)$ is the *Soft bit value* [15] of the CBMS(\mathbf{p}, σ) channel and $\mathbf{p}_{(\lambda, \rho)}^*$ is as in Proposition 4. Then, $\underline{\mathcal{S}}_{(\lambda, \rho)} \subset \mathcal{R}_{(\lambda, \rho)}$.

Discussion This follows from the one-dimensional non-iterative bound based on the *Soft bit value* given in [15].

Figure 4 shows the inner bounds for the two code ensembles considered before. We note here that the degradation inner bound and the soft bit inner bound are tight on the \mathbf{p} -axis, i.e. on the \mathbf{p} -axis, the $\underline{\mathcal{D}}$ and $\underline{\mathcal{S}}$ bounds meet the $\bar{\mathcal{D}}$ bound. The set $\underline{\mathcal{B}}_{(\lambda, \rho)} \cup \underline{\mathcal{H}}_{(\lambda, \rho)} \cup \underline{\mathcal{D}}_{(\lambda, \rho)} \cup \underline{\mathcal{S}}_{(\lambda, \rho)}$ is therefore an inner bound to the decodable region $\mathcal{R}_{(\lambda, \rho)}$. Note that in the case of the (3, 6) regular code ensemble, the soft bit inner bound is tighter than all other inner bounds. This, however, is not true in the case of the optimized rate-0.9 code ensemble (See Figure 4).

C. Decodable region

The actual decodable region was found using density evolution. By fixing σ , we are guaranteed by Lemma 2 the existence of a threshold \mathbf{p}_σ^* – the largest \mathbf{p} for which the decoder gives a zero error. The boundary of $\mathcal{R}_{(\lambda, \rho)}$ is therefore estimated by finding the \mathbf{p}_σ^* for a fixed set of σ values within the range $[0, \sigma_{(\lambda, \rho)}^*]$, where $\sigma_{(\lambda, \rho)}^*$ is as in Proposition 4. This is shown in Figure 5 for our example code ensembles. We conjecture that the decodable region of a code ensemble, like most of the bounds we have obtained, is a *convex* subset of the channel space \mathcal{S} .

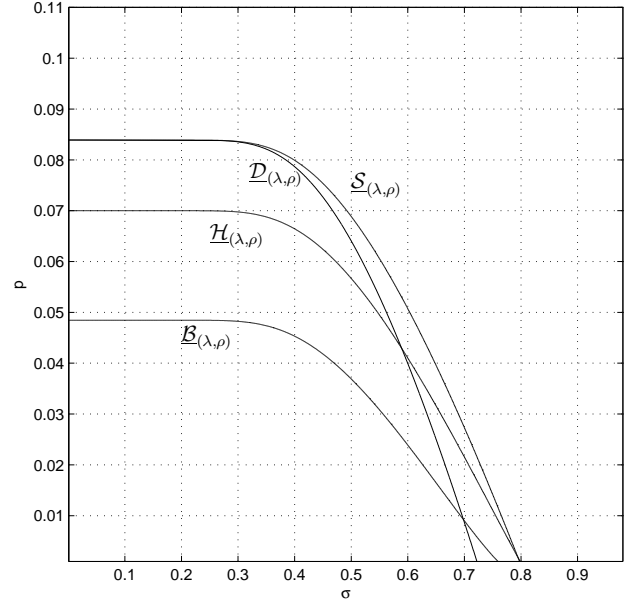
IV. MESSAGE-PASSING

In this section, we propose two alternative message-passing schemes to the BP decoder. The schemes and the motivation for considering them are discussed below.

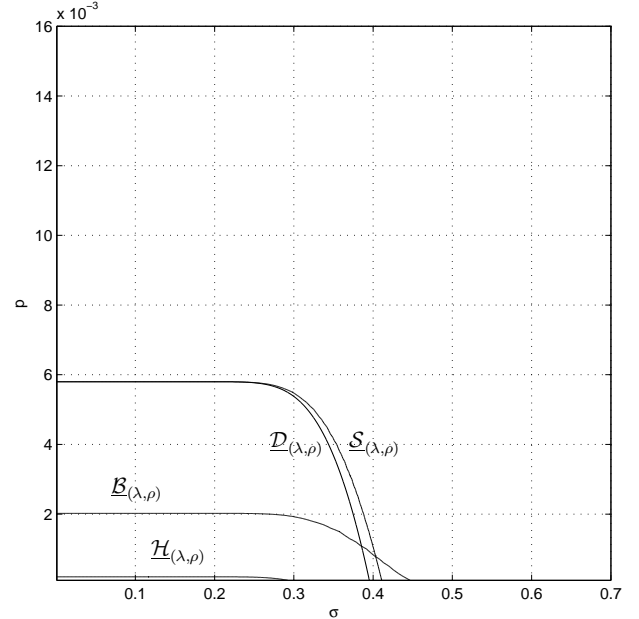
A. Decoding schemes

Hard Decision decoder (HD): Here we threshold the output of the CBMS(\mathbf{p}, σ) channel and consider the channel to now function as a BSC with crossover probability $\mathbf{p}' = \mathbf{p} \star Q\left(\frac{1}{\sigma}\right)$ where \star and $Q(\cdot)$ are as defined in Proposition 7. We then perform BP for this modified BSC. The rationale is that a good code for the BSC should be able to tackle the written-in errors well.

Gaussian Noise decoder (GN): In this case, we have a decoder that ignores the first subchannel and performs BP under the assumption that the channel is a simple BAWGN channel. Analysing the performance of this decoder is useful, e.g. in the case of magnetic recording, to understand the penalty paid in naively assuming that the information written on to a disk is error-free. Note that since we ignore the first



(a) (3, 6) regular code ensemble.



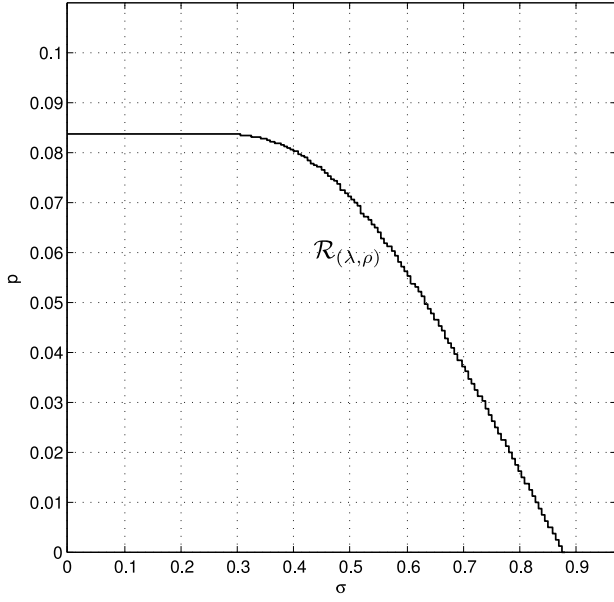
(b) Optimized rate 0.9 code ensemble.

Fig. 4. Inner bounds for the decodable region $\mathcal{R}_{(\lambda, \rho)}$.

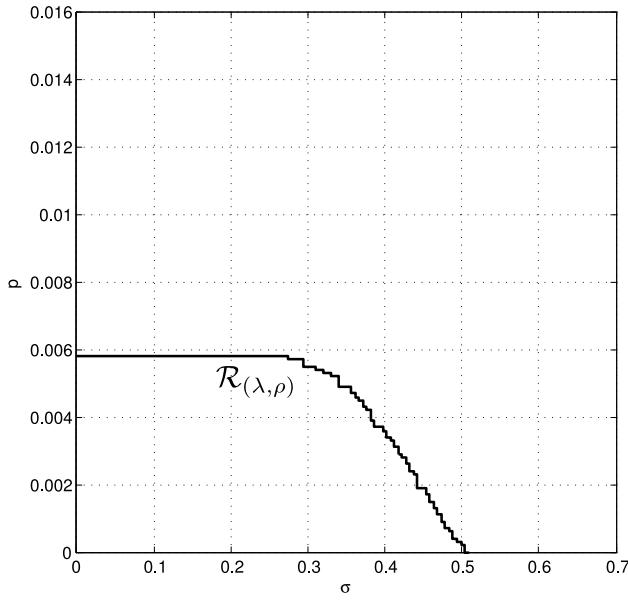
subchannel here, the estimation of \mathbf{p} is not necessary, and therefore the decoder is slightly less complex than the other two decoders in this respect.

B. Decodable regions

The degradation inner bound $\underline{\mathcal{D}}$ of the BP decoder gives the decodable region for the HD decoder. This is true because the construction in the proof of Proposition 7 is the same as the operation performed in the HD decoder.



(a) (3, 6) regular code ensemble.



(b) Optimized rate 0.9 code ensemble.

Fig. 5. BP Decodable region $\mathcal{R}_{(\lambda, \rho)}$.

For the GN decoder, since the decoder assumes a wrong channel model, we use density evolution with the LLR calculated as $l = 2y/\sigma^2$, where y is the channel output conditioned on the transmission of a 1 –

$$f_{Y|X}(y|1) = \frac{1}{\sqrt{2\pi\sigma^2}} \left\{ (1-p) \exp\left(-\frac{(y-1)^2}{2\sigma^2}\right) \right\} + \frac{1}{\sqrt{2\pi\sigma^2}} \left\{ p \exp\left(-\frac{(y+1)^2}{2\sigma^2}\right) \right\}.$$

In this case, we can make no claim of the monotonicity in σ of the decoder performance. The decodable region for the GN decoder is found as in the case of the BP decoder, however

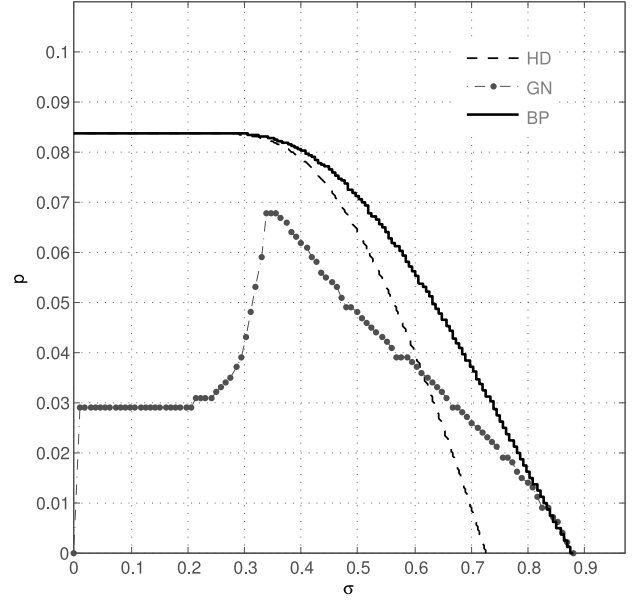


Fig. 6. Decodable regions for the BP, HD, and GN decoders for (3, 6) regular code ensemble.

by using the modified LLR density.

In Figure 6, we give the decodable regions for the HD, GN and BP decoders for the (3, 6) regular code ensemble. We make two observations from this figure – first, the non-monotonicity of the performance of the GN decoder apparent from the shape of its decodable region, and second, the similarity in the performance of the HD and BP decoders for small σ (large SNR) and large p . Also note that the decodable region of the GN decoder is another inner bound to the decodable region of the BP decoder.

The non-monotonicity of the GN decoder in σ , for large enough p is because the decoder in this case is being fooled into believing that the channel is reliable when it is not. For large p and small σ , the performance of the HD decoder and the BP decoder coincide because the CBMS channel in this case is very similar to the BSC, i.e. the behaviour of the cascaded channel is dominated by the behavior of the first subchannel. Also, as expected, the HD and the GN decoders are as good as the BP decoder when the channel is dominated by the BSC and the BAWGNC respectively.

V. EXPERIMENTAL RESULTS

In this section, we shall explore the performance of binary LDPC codes on the CBMS(p, σ) channel with the three different message-passing schemes proposed in earlier sections. A rate-1/2 binary LDPC code of blocklength 4096 bits that was randomly sampled (with multiple edges between nodes avoided) from the Gallager (3, 6) regular ensemble was used to estimate the decoder performance. The values used for p ranged from 1% through 5%.

Since the CBMS(p, σ) channel is memoryless, all the decoding schemes have the same complexity and this complexity scales as $O(Ln(d_v q + \bar{r} d_c q \log_2 q))$ where L is the maximum number of iterations performed, n is the blocklength of the

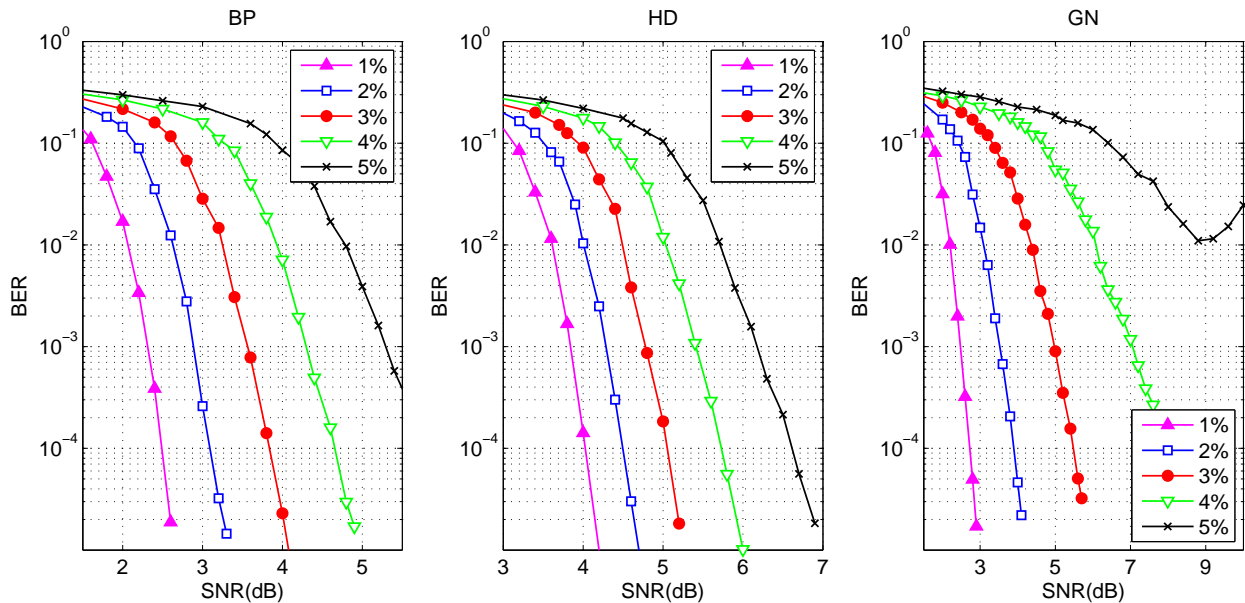


Fig. 7. Performance of the decoders for increasing p .

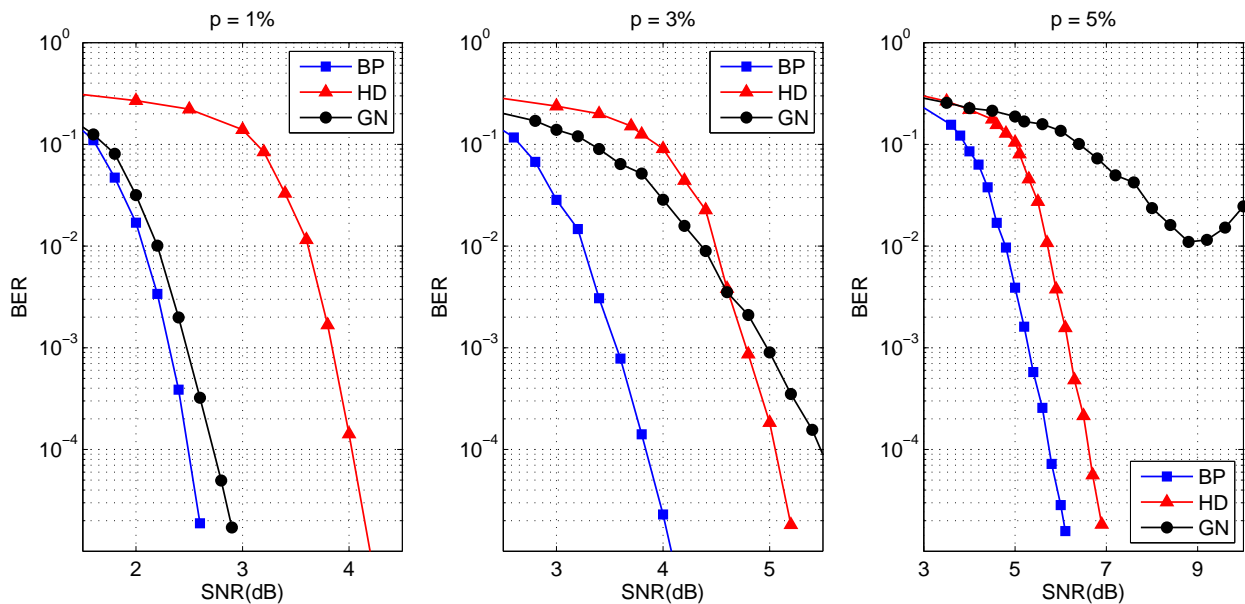


Fig. 8. Performance comparison of the BP, HD, and GN decoders for different p values.

code, d_v and d_c are the maximum variable and check node degrees respectively in the Tanner graph of the code, \bar{r} is the *normalized redundancy* of the code, given as $\bar{r} = 1 - r$ where r is the design rate. q is the size of the Galois field over which the code is defined ($q = 2$).

Figure 7 shows the performance of each decoder over the range of p values. In Figure 8, we compare the three decoders for different values of p . We see from Figure 8 that the BP decoder outperforms both the HD and the GN decoders, as expected. However, with increasing p , the HD decoder performs better than the GN decoder at high SNR values, i.e. as the channel becomes more like the BSC (small σ , large

p), the HD decoder handles the channel better than the GN decoder. Note that beyond a certain p , the performance of the GN decoder is non-monotonic in σ , e.g. when $p = 5\%$, the BER first reduces and then increases with increasing SNR (See Figure 7). Also notice that the gap between the BP and the HD decoder (Figure 8) at a high SNR reduces as p increases, going from ≈ 1.5 dB when $p = 1\%$ to ≈ 0.8 dB when $p = 5\%$. These agree with the observations made in Section IV-B from the decodable regions of these decoders.

VI. GOOD CODES FOR THE CBMS(p, σ) CHANNEL

From Figure 3(b), we see that the optimized rate-0.9 code comes very close to achieving capacity on the BAWGNC –

with a threshold of $\sigma^* \approx 0.5089$ while capacity is $\sigma^C \approx 0.5113$. However, it falls well short of the capacity on the BSC. The threshold for this code on the BSC was observed to be $p^* \approx 0.0058$ while a capacity of 0.9 bits per channel use was achieved by a channel with $p^C \approx 0.01298$. This suggests that a code optimized for the BAWGNC might be far from optimal on the BSC. In Figure 9, we show the decodable regions of the BP decoder for two code ensembles of rate 0.75, one optimized for the BAWGNC $C^g = (0.403522x^{14} + 0.0007697x^6 + 0.0741103x^5 + 0.115054x^4 + 0.000008x^3 + 0.221315x^2 + 0.185221x, 0.5x^{17} + 0.5x^{16})$ with the decodable region \mathcal{R}_g , and another optimized for the BSC $C^s = (0.419558x^{29} + 0.00213211x^8 + 0.246425x^6 + 0.0721407x^5 + 0.147928x^2 + 0.111817x, x^{23})$ with decodable region \mathcal{R}_s . These optimized codes were obtained from [17].

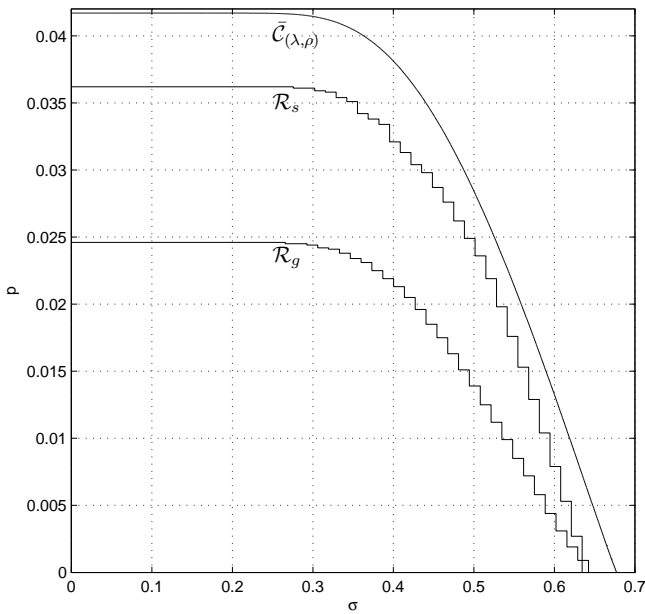


Fig. 9. Decodable region estimates for the two optimized code ensembles C^g and C^s of rate 0.75.

Also shown in the figure is the capacity outer bound for the decodable region of a code of rate 0.75. The ideal rate-0.75 code for the $\{\text{CBMS}(\rho, \sigma)\}$ family has $\bar{C}_{(\lambda, \rho)}$ as its decodable region.

We see from Figure 9 that the code optimized for the BSC performs better (is closer to the capacity bound) than the code optimized for the BAWGNC except near the σ -axis, i.e. the BAWGNC optimized code is superior only when the channel is dominated by the BAWGN subchannel. This suggests that a good strategy to obtain good codes for the $\text{CBMS}(\rho, \sigma)$ channel is to optimize a code for the BSC, rather than optimizing for the BAWGNC. A better scheme would be to optimize the degree distributions for a fixed rate code over both the BAWGNC and BSC simultaneously, which is clearly a more complex optimization problem.

VII. CONCLUSION

We have introduced a new class of BMS channels that model many scenarios including the BPM recording channel.

We analyzed the theoretical decodable regions of LDPC codes under BP decoding over the family of $\text{CBMS}(\rho, \sigma)$ channels by giving inner and outer bounds to the decodable region based on channel parameters like the entropy, the Bhattacharyya constant, the Soft bit value and the capacity, and also based on the channel ordering introduced by degradation. We also numerically estimated the decodable regions for three proposed message-passing decoders, including the BP decoder using density evolution.

We conducted performance estimation for a rate-1/2 (3, 6)-regular LDPC code of blocklength 4096 bits with the three proposed message-passing schemes and showed the decoder characteristics suggested by theory. In particular, we showed that ignoring the BSC (as in the GN decoder) can result in a large penalty in performance, more so when the channel SNR is high. By looking at codes optimized for the BSC and BAWGNC, we noted that optimizing a code over the BSC works better than optimizing for the BAWGNC. Both these suggest that the first subchannel, the BSC, plays a very key role in the $\text{CBMS}(\rho, \sigma)$ channel, and any good code construction for the channel should take into account its effects.

REFERENCES

- [1] R. G. Gallager, *Low Density Parity Check Codes*. Cambridge, Massachusetts: MIT Press, 1963.
- [2] D. MacKay and R. Neal, "Near Shannon limit performance of low density parity check codes," *Electronics Letters*, vol. 33, no. 6, pp. 457–458, Mar 1997.
- [3] T. Richardson and R. Urbanke, *Modern Coding Theory*. Cambridge University Press, 2008.
- [4] M. Luby, M. Mitzenmacher, M. Shokrollahi, and D. Spielman, "Efficient erasure correcting codes," *IEEE Trans. Inform. Theory*, vol. 47, no. 2, pp. 569–584, Feb 2001.
- [5] A. Amraoui, "Asymptotic and finite-length optimization of LDPC codes," Ph.D. dissertation, EPFL, Switzerland, 2006.
- [6] S.-Y. Chung, J. Forney, G.D., T. Richardson, and R. Urbanke, "On the design of low-density parity-check codes within 0.0045 dB of the Shannon limit," *Communications Letters, IEEE*, vol. 5, no. 2, pp. 58–60, Feb 2001.
- [7] S.-Y. Chung, "On the construction of some capacity achieving coding schemes," Ph.D. dissertation, MIT, Cambridge, Massachusetts, 2000.
- [8] T. Richardson and R. Urbanke, "The capacity of low-density parity-check codes under message-passing decoding," *IEEE Trans. Inform. Theory*, vol. 47, no. 2, pp. 599–618, Feb 2001.
- [9] C. A. Desoer, "Communication through channels in cascade," Ph.D. dissertation, MIT, Cambridge, Massachusetts, 1953.
- [10] R. Silverman, "On binary channels and their cascades," *IRE Trans. Inform. Theory*, vol. 1, no. 3, pp. 19–27, December 1955.
- [11] M. Simon, "On the capacity of a cascade of identical discrete memoryless nonsingular channels (corresp.)," *IEEE Trans. Inform. Theory*, vol. 16, no. 1, pp. 100–102, Jan 1970.
- [12] A. Kiely and J. Coffey, "On the capacity of a cascade of channels," *IEEE Trans. Inform. Theory*, vol. 39, no. 4, pp. 1310–1321, Jul 1993.
- [13] B. Livshitz, A. Inomata, H. N. Bertram, and V. Lomakin, "Semi-analytical approach for analysis of BER in conventional and staggered bit patterned media," *IEEE Trans. Magnetics (Accepted)*, 2009.
- [14] A. Khandekar and R. J. McEliece, "A lower bound on the iterative decoding threshold of irregular LDPC code ensembles," in *Proc. 36th Conf. Information Sciences and Systems*, Princeton, New Jersey, Mar. 2002.
- [15] C.-C. Wang, S. R. Kulkarni, and H. V. Poor, "Finite-dimensional bounds on \mathbb{Z}_m and binary LDPC codes with belief propagation decoders," *IEEE Trans. Inform. Theory*, vol. 53, no. 1, pp. 56–81, Jan. 2007.
- [16] I. Sutskov, S. Shamai, and J. Ziv, "Extremes of information combining," *IEEE Trans. Inform. Theory*, vol. 51, no. 4, pp. 1313–1325, April 2005.
- [17] A. Amraoui and R. Urbanke, "LDPCOpt," Accessed June 29, 2009, <http://ipgdemos.epfl.ch/ldpcopt/>.